Eur. J. Biochem. 145, 531–542.
Hirohashi, S., Clausen, H., Nudelman, E., Inoue, H., Shimosato, Y., & Hakomori, S. (1986) *J. Immunol. 136*, 4163–4168.
Kannagi, R., Nudelman, E., Levery, S. B., & Hakomori, S. (1982) *J. Biol. Chem. 257*, 14865–14874.
Kannagi, R., Stroup, R., Cochran, N. A., Urdal, D. L., Young, W. W., Jr., & Hakomori, S. (1983a) *Cancer Res. 43*, 4997–5005.
Kannagi, R., Roelcke, D., Peterson, K. A., Okada, Y., Levery, S. B., & Hakomori, S. (1983b) *Carbohydr. Res. 120*, 143–157.
Köhler, G., & Milstein, C. (1975) *Nature (London) 256*, 495–497.
Laine, R. A. (1980) *Int. Congr. Pure Appl. Chem. [Proc.], 27th*, 193–198.
Levery, S. B., & Hakomori, S. (1986) *Methods Enzymol.* (in press).
Lindberg, B., & Lönngren, J. (1978) *Methods Enzymol. 50*, 3–33.
Magnani, J. L. (1985) *Anal. Biochem. 150*, 13–17.
Magnani, J. L., Smith, D. F., & Ginsburg, V. (1980) *Anal. Biochem. 109*, 399–402.
McKibbin, J. M., Spencer, W. A., Smith, E. L., Mansson, J.-E., Karlsson, K.-A., Samuelsson, B. E., Li, Y.-T., & Li, S. C. (1982) *J. Biol. Chem. 257*, 755–760.
McNeil, M., & Albersheim, P. (1977) *Carbohydr. Res. 56*, 239–248.
Stellner, K., Saito, H., & Hakomori, S. (1973) *Arch. Biochem. Biophys. 155*, 464–472.
Takasaki, S., Yamashita, K., & Kobata, A. (1978) *J. Biol. Chem. 253*, 6086–6091.
Tang, P. W., Gooi, H. C., Hardy, M., Lee, Y. C., & Feizi, T. (1985) *Biochem. Biophys. Res. Commun. 132*, 474–480.
Watanabe, K., & Arao, Y. (1981) *J. Lipid Res. 22*, 1020–1024.
Watanabe, K., Laine, R. A., & Hakomori, S. (1975) *Biochemistry 14*, 2725–2733.
Watkins, W. M. (1980) *Adv. Hum. Genet. 10*, 1–136.
Yu, R. K., & Ledeen, R. W. (1972) *J. Lipid Res. 13*, 680–686.

Electrostatic Analysis of the Interaction of Cytochrome *c* with Native and Dimethyl Ester Heme Substituted Cytochrome b_5†

Marcia R. Mauk and A. Grant Mauk*
Department of Biochemistry, University of British Columbia, Vancouver, British Columbia V6T 1W5, Canada
Patricia C. Weber and James B. Matthew*
Central Research & Development Department, E. I. du Pont de Nemours & Company, Experimental Station, Wilmington, Delaware 19898

Received February 25, 1986; Revised Manuscript Received May 21, 1986

ABSTRACT: The stability of the complex formed between cytochrome *c* and dimethyl ester heme substituted cytochrome b_5 (DME-cytochrome b_5) has been determined under a variety of experimental conditions to evaluate the role of the cytochrome b_5 heme propionate groups in the interaction of the two native proteins. Interaction between cytochrome *c* and the modified cytochrome b_5 was found to produce a difference spectrum in the visible range that is very similar to that generated by the interaction of the native proteins and that can be used to monitor complex formation between the two proteins. At pH 8 [25 °C (HEPPS), I = 5 mM], DME-cytochrome b_5 and cytochrome *c* form a 1:1 complex with an association constant K_A of 3 (1) $\times 10^6$ M^{-1}. This pH is the optimal pH for complex formation between these two proteins and is significantly higher than that observed for the interaction between the two native proteins. The stability of the complex formed between DME-cytochrome b_5 and cytochrome *c* is strongly dependent on ionic strength with K_A ranging from 2.4×10^7 M^{-1} at I = 1 mM to 8.2×10^4 M^{-1} at I = 13 mM [pH 8.0 (HEPPS), 25 °C]. Calculations for the native, trypsin-solubilized form of cytochrome b_5 and cytochrome *c* confirm that the intermolecular complex proposed by Salemme [Salemme, F. R. (1976) *J. Mol. Biol. 102*, 563] describes the protein–protein orientation that is electrostatically favored at neutral pH. For the interaction between cytochrome *c* and the less negatively charged DME-cytochrome b_5, an alternative interaction geometry was identified that is electrostatically isoenergetic with the original model at neutral pH. This alternative complex involves different amino acid residues at the intermolecular interface and positions the heme prosthetic groups in a non-coplanar orientation. Further electrostatic calculations indicate that the difference in stability of these complexes for either pair of proteins is a kilocalorie or less depending on pH. Therefore, we conclude that the nature of protein–protein complexes formed is in part dependent on the solution conditions and that an ensemble of protein–protein complexes exists in solution as precursors to an efficient electron-transfer geometry.

Several studies have shown that rates of electron transfer between proteins that function as physiological electron-transfer partners depend strongly on ionic strength. These observations have led to the conclusion that electrostatic interactions are important in facilitating the formation of a productive protein–protein electron-transfer complex. The reaction between cytochrome b_5 and cytochrome *c* is a particularly attractive model for studying the electrostatic interactions involved in protein–protein recognition during

† This research was supported by Grant GM-28834 from the National Institutes of Health (to A.G.M.). A preliminary account of this work was presented at the Annual Meeting of the Federation of American Societies for Experimental Biology, Anaheim, CA, April 1985 (Mauk et al., 1985).

0006-2960/86/0425-7085$01.50/0

protein–protein electron-transfer reactions because the three-dimensional structures of both proteins are known (Mathews et al., 1979; Takano & Dickerson, 1981a,b). Based in part on these structures, a detailed hypothetical model has been proposed for the complex that forms between the two proteins immediately prior to electron transfer (the precursor complex) (Salemme, 1976).

This structural model incorporates complementary salt linkages between negatively charged side chains on cytochrome b_5 and lysyl residues of cytochrome *c* (Salemme, 1976). Subsequently, spectroscopic measurements established that these proteins form a 1:1 complex, the stability of which is extremely sensitive to the pH and ionic strength of the solution (Mauk et al., 1982). Experimental results from several laboratories (Ng et al., 1977; Stonehuerner et al., 1979; Eley & Moore, 1983; McLendon et al., 1985) have provided supporting evidence for several of the intermolecular electrostatic interactions proposed in this model.

One notable structural feature of this hypothetical complex that has not been experimentally examined is the involvement of one of the cytochrome b_5 heme propionate groups in a salt link to a lysyl residue on the surface of cytochrome *c*. We have now examined the role of the cytochrome b_5 heme propionates in complex formation by measuring the association constants for the interaction of cytochrome *c* with trypsin-solubilized cytochrome b_5 and with the corresponding dimethyl ester heme substituted form of cytochrome b_5 (DME-cytochrome b_5) (Reid et al., 1984). The reduction of the net negative charge on cytochrome b_5, in the center of the protein surface proposed to interact with cytochrome *c*, was expected to reduce both the association constant and ionic strength dependence of its interaction with cytochrome *c*. Neither expectation was fulfilled. To interpret these findings, we have used computer graphic modeling, computed electrostatic potential surfaces, and calculated electrostatic free energies of stabilization to show that the observed experimental results are consistent with the occurrence in solution of an electrostatically mediated ensemble of protein–protein complexes.

Experimental Procedures

The tryptic fragment of bovine liver cytochrome b_5 and its dimethyl ester heme substituted derivative were prepared as described previously (Reid & Mauk, 1982; Reid et al., 1984). Horse heart cytochrome *c* was obtained from Sigma (Type VI) and used without further purification. HEPPS[1] and HEPES were obtained from Calbiochem. Phosphate buffers were prepared as described previously (Mauk et al., 1982). HEPPS and HEPES buffers of known ionic strength were prepared by adding the appropriate solid to dilute solutions of sodium hydroxide (prepared from standardized stock solutions) to obtain the required pH.

Protein concentrations were determined, difference spectra were obtained, spectrophotometric titrations were performed, and stability constants were calculated as previously described (Mauk et al., 1982).

The p*K* values for ionizable amino acid residues in the proteins of interest and the electrostatic potential surfaces for the cytochromes and their complexes were calculated according to the solvent accessibility discrete charge formalism. This approach takes into account all charged atoms in the protein and scales the local dielectric constant of each charged group according to its solvent-accessible surface area (Matthew & Richards, 1982; Matthew, 1985). In these computations, it is assumed that for each pH and ionic strength the unique protein charge array confers an electrostatic potential at site i causing the apparent pK, pK_i, to deviate from the intrinsic pK of the site, pK_{int}. The pK_i of almost every group is found to vary with pH, and it is convenient to define the parameter p$K_{1/2}$ for a group, this being the pH at which a particular group is half-titrated. In the absence of electrostatic interaction, $\sum_{j \neq i} pK_{ij}$ goes to zero, the pK_{int} equals p$K_{1/2}$, and the variations of pK_i with pH disappear.

Atomic coordinates for the soluble fragment of bovine liver cytochrome b_5 (Mathews et al., 1972) were taken from the Brookhaven Protein Data Bank (Bernstein et al., 1977). The residue numbering system of Mathews et al. (1972) was retained although only residues 3–84 of the crystallographic structure were used in the modeling and computational studies. This slightly shorter protein sequence is consistent with the trypsin-cleavage results, which show cleavage sites between residues 2 and 3 and between residues 84 and 85 of lipase-solubilized cytochrome b_5 used in the crystallographic studies (Strittmatter & Ozols, 1966). Coordinates for tuna ferricytochrome *c* (Swanson et al., 1977) were used as a structural model for horse heart cytochrome *c*. The amino acid sequences of these cytochromes *c* differ by a single residue in length (Dayhoff, 1972) and share close structural homology (Salemme, 1977).

Protein–protein interactions were studied by interactive computer graphic techniques similar to those reported previously (Weber & Tollin, 1985). The proteins were docked to within 3 Å of van der Waals contact by maximizing the overlap of their complementary electrostatic potential surfaces. Individual proteins were then independently rotated and translated as rigid bodies until a favorable geometry for closest approach was found; rearrangement of side chains involved in intermolecular salt linkages was allowed to facilitate docking and to maximize favorable interactions between oppositely charged atoms. Interatomic distances between all atoms in each protein were checked to ensure that no van der Waals overlaps occurred at the intermolecular interface.

Results

Protein–Protein Association Constants. The difference spectra resulting from the interaction of cytochrome *c* with DME-cytochrome b_5 and with native cytochrome b_5 are compared in Figure 1. Similar spectra obtained in the Soret region as a function of pH are illustrated in Figure 2. The difference absorbance maxima produced on mixing the two native proteins occur at 527 and 562 nm while for the interaction between DME-cytochrome b_5 and cytochrome *c* they occur at 527 and 565 nm. These difference spectra represent a change in absorbance of approximately 1.3% at 527 nm.

The absorbance difference illustrated in Figure 1 was used as a measure of complex formation to produce titration curves similar to those obtained previously for the native proteins (Mauk et al., 1982). The pH and ionic strength dependencies of complex stability for native cytochrome b_5 and DME-cytochrome b_5 with cytochrome *c* are shown in Figures 3 and 4, respectively. The results for the native proteins in HEPES and HEPPS are indistinguishable from those obtained in phosphate buffers (Mauk et al., 1982) and indicate that specific anion effects are not responsible for the difference in optimal pH for complex formation.

Electrostatic Calculations and Computer Graphic Modeling. Two approaches have been taken to understand the role that complementary charge interaction plays in the observed

[1] Abbreviations: HEPPS, *N*-(2-hydroxyethyl)piperazine-*N*′-3-propanesulfonic acid; HEPES, *N*-(2-hydroxyethyl)piperazine-*N*′-2-ethanesulfonic acid.

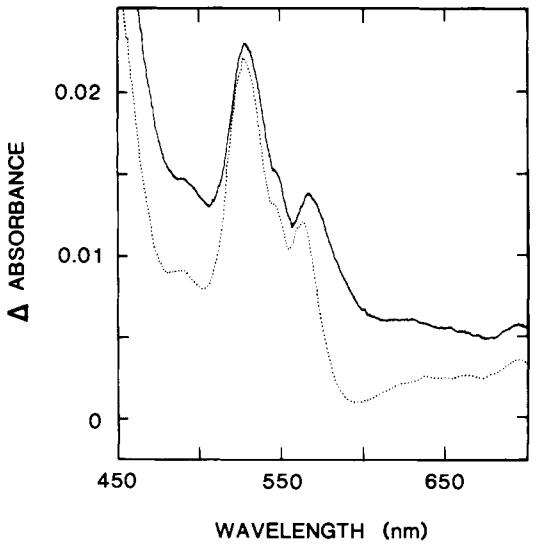

FIGURE 1: Difference spectra resulting from the interaction of cytochrome *c* with cytochrome b_5 (···) and with DME-cytochrome b_5 (—) [pH 7.5 (phosphate), I = 5 mM, 25 °C]. The concentrations after mixing were 96.6 μM cytochrome b_5, 97.6 μM DME-cytochrome b_5, and 94.6 μM cytochrome *c* in each case. Spectra were obtained with matched tandem cuvettes having path lengths of 0.874 cm. Each spectrum has been corrected for the instrument base line.

protein association behavior. In the first of these, the data were fit to an equation whose variables are conceptually related to an interaction model. The second approach involved the application of computer graphic and electrostatic calculations based on the available protein crystal structures to generate predictions concerning protein–protein association for comparison with the experimental observations.

Following Wherland and Gray (1976), the data for the ionic strength dependence of K_a were fit to a form of the Debye–Hückel equation, which consists of a two-parameter [ln K_a(inf) and Z_1Z_2] model whose values of best fit are assumed to represent the protein–protein association constant at infinite ionic strength (i.e., no Coulombic component to binding) and the product of the effective charges on the two interacting proteins, respectively. Values of ln K_a(inf) calculated from the cytochrome *c*–cytochrome b_5 data (see Figure 4) are 6.6 ± 0.7 at pH 7.0 and 6.8 ± 1.1 at pH 7.5. These values are comparable to the cytochrome b_5–cytochrome *c* value of 6.2 ± 1.3 at the optimal pH of 8.0. The corresponding Z_1Z_2 values of −56 ± 6, −63 ± 12 for cytochrome *c*–cytochrome b_5 and −73 ± 13 for cytochrome *c*–DME-cytochrome b_5 suggest that the charge product for the protein–protein complexes involved is not reduced by the elimination of the two propionate charges.

Table I: Cytochrome b_5 Residues with p$K_{1/2}$ Values Calculated To Be between 6.5 and 8.5[a]

residue	isolated protein[b]	Fe–Fe distance for cyt b_5 bound to cyt *c* 17.9 Å	25.9 Å
native cyt b_5			
His-80	6.6	6.6	6.5
His-26	7.5	7.2	7.3
Ala-3	8.0	8.0	8.0
DME-cyt b_5			
His-80	6.6	6.6	6.5
His-26	7.3	7.0	7.6
Ala-3	8.0	8.0	8.0

[a] Ionic strength = 4 mM. [b] Residue numbers are based on the system of Mathews et al. (1972). The cytochrome b_5 tryptic cleavage sites occur between residues 2 and 3 and between residues 84 and 85 of the lipase-solubilized cytochrome used in the crystallographic studies. The resulting protein contains 82 amino acid residues. Cytochrome *c* has no titratable groups in this range.

Electrostatic calculations based on the three-dimensional protein structures were carried out to determine the molecular basis for the similar behavior observed for the native and charge-modified cytochrome b_5 in their interactions with cytochrome *c*. At any given pH and ionic strength, an effective pK value, pK_i, is calculated for the ionizable groups of each protein or protein–protein complex by summing all pairwise Coulombic interactions within the isolated protein (Matthew, 1985; Matthew et al., 1983; Matthew & Richards, 1982). Experimental hydrogen ion titrations and the electrostatic calculations both indicate that no cytochrome *c* groups titrate in the pH range of 6–8 (Matthew et al., 1978). The calculated proton dissociation constants for residues in isolated native cytochrome b_5 and DME-cytochrome b_5 with titration midpoints, p$K_{1/2}$, between pH 6 and 8.5 are given in Table I. The electrostatic effect of propionate esterification on ferricytochrome b_5 predicted by these calculations is the reduction of the p$K_{1/2}$ of His-26 from 7.5 to 7.3. In the cytochrome b_5 structure, His-26 is salt-linked to Glu-59, and elimination of

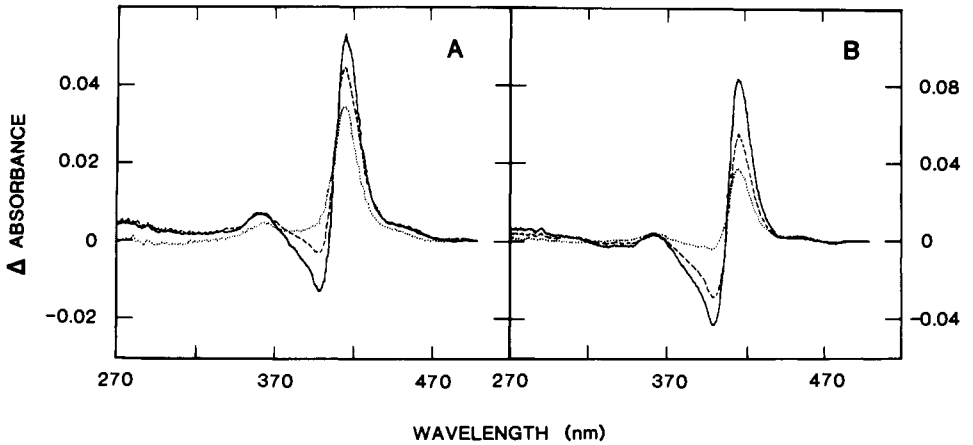

FIGURE 2: Effect of pH on difference spectra resulting from the interaction of cytochrome *c* with cytochrome b_5 or DME-cytochrome b_5 (I = 5 mM, 25 °C, HEPPS buffer except where noted). Spectra were normalized to a concentration after mixing of 9.84 μM cytochrome b_5 or DME-cytochrome b_5. (A) Difference spectrum produced on mixing cytochrome b_5 with cytochrome *c*. The concentration of cytochrome *c* after mixing was 11.07 μM at pH 7.0 (···, HEPES buffer), 10.80 μM at pH 7.5 (---), and 11.15 μM at pH 7.75 (—). (B) Difference spectrum produced on mixing DME-cytochrome b_5 with cytochrome *c*. The concentration of cytochrome *c* after mixing was 10.58 μM at pH 7.5 (···), 10.86 μM at pH 8.0 (---), and 11.25 μM at pH 8.5 (—). Spectra were obtained with matched tandem cuvettes with path lengths of 0.874 cm as described previously (Mauk et al., 1982).

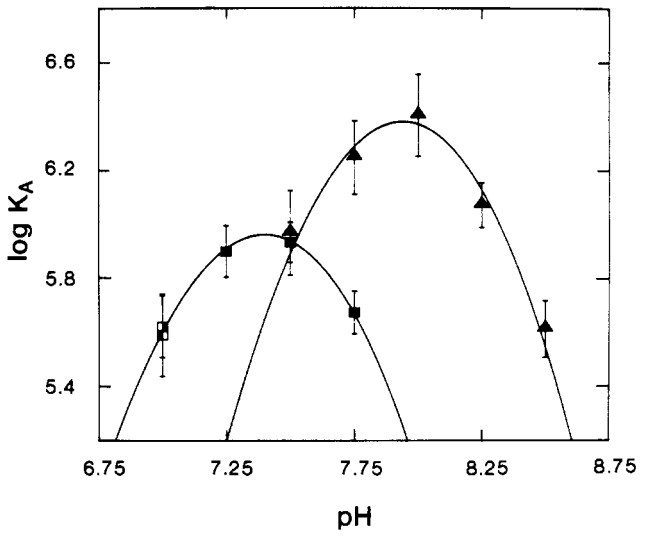

FIGURE 3: pH dependence of K_A for complex formation between cytochrome c and either native cytochrome b_5 or DME-cytochrome b_5 (25 °C, I = 5 mM): cytochrome b_5–cytochrome c complex in HEPPS (■), HEPES (◨), and phosphate (◧) buffer; DME-cytochrome b_5–cytochrome c complex in HEPPS buffer (▲).

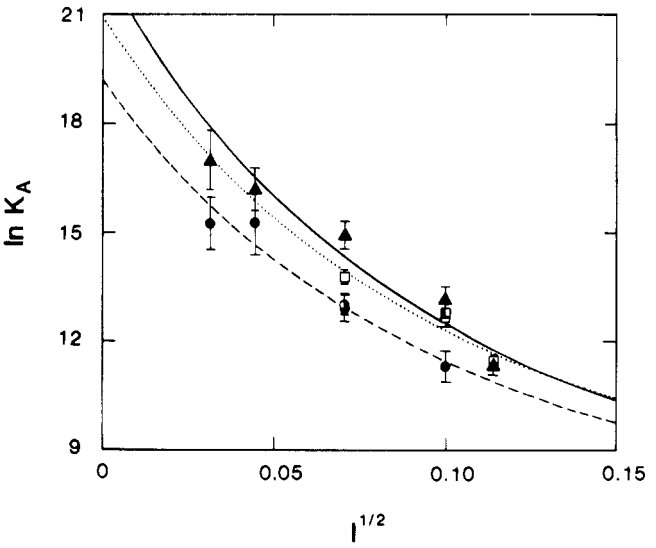

FIGURE 4: Ionic strength dependence of K_A for complex formation between cytochrome c and either native cytochrome b_5 or DME-cytochrome b_5: cytochrome b_5–cytochrome c (pH 7.5, 25 °C) in HEPPS (□···□) or phosphate (◧···◧); cytochrome b_5–cytochrome c (pH 7.0, 25 °C) in phosphate (●---●) or HEPES (◑---◑); DME-cytochrome b_5–cytochrome c [pH 8.0 (HEPPS), 25 °C] (▲—▲). The lines are weighted least-squares fits of the data to the Wherland–Gray equation (Wherland & Gray, 1976).

the heme propionate charges destabilizes this interaction. Other residues titrating in the neutral pH range, the amino terminus (Ala-3) and His-80, are not predicted to be perturbed by esterification of the heme propionates.

Electrostatic potential surfaces, 4 kT, calculated from the computed charge distributions for native and modified cytochrome b_5 at pH 7.6 are shown in Figure 5A. The electrostatic potential outside the protein's solvent accessibility surface is exclusively negative at this energy level. The absence of contoured potential about large areas of the protein's surface indicates that the positive and negative charges on these surfaces are symmetrically disposed. Removal of the heme propionates does, however, substantially reduce the extent of the negative potential and actually shifts its center away from the heme edge. The electrostatic potential about cytochrome c, also shown in Figure 5A, is positive in the vicinity of the heme edge (Matthew et al., 1983). Figure 5B shows the expected orientation of cytochrome c relative to the electrostatic potential surfaces of isolated native and modified cytochrome b_5.

Figure 6A shows a molecular model for the interaction of DME-cytochrome b_5 with cytochrome c. The molecules were aligned to maximize the overlap of their individual electrostatic potential surfaces. The proteins were then rigidly rotated and translated to remove any intermolecular van der Waals overlap. Only the conformations of charged side chains were altered to facilitate formation of intermolecular salt linkages. Figure 6B shows the molecular model for native cytochrome b_5 and cytochrome c complexed [as originally proposed by Salemme (1976)] to maximize Coulombic interaction and minimize interprosthetic group distance in a coparallel arrangement. Both complexes involve considerable overlap between the oppositely charged electrostatic potentials of the isolated proteins (parts A and B of Figure 5). Four intermolecular salt linkages also stabilize each complex. However, comparison of the models shown in Figures 5 and 6 readily shows the differences in relative molecular orientation. The complexes differ in their interprosthetic group geometry in two ways. The heme iron to heme iron separation is increased to 25.9 Å in the complex between the native proteins. The heme moieties of the DME-cytochrome b_5–cytochrome c complex are no longer coplanar as in the complexed native proteins but are oriented at approximately 127.4° to each other.

In Figure 7, the calculated electrostatic stabilization is given as a function of pH for the interaction of native and modified cytochrome b_5 with cytochrome c for both of the interaction geometries shown in Figure 6. The heme edge to heme edge complex, Figure 6B, is predicted to be relatively independent of pH for both native and esterified cytochrome b_5 (Figure 7, curves 1 and 2, respectively); however, removal of the propionate charges reduces its electrostatic stability by about 1.1 kcal/mol, −6.75 to −5.6 kcal/mol. In the off-edge complex geometry (Figure 6A) the interaction of cytochrome c with both native and modified cytochrome b_5 is calculated to be pH-dependent (Figure 7, curves 3 and 4, respectively). The computed pH dependence for this geometry is attributable to the proximity of the intermolecular protein interface to the His-26/Glu-59 salt bridge within cytochrome b_5. Over the pH range of 6.5–8.0, the heme edge complex of cytochrome c with unmodified cytochrome b_5 is preferred, but at pH 8.0–8.5, the predicted electrostatic interaction between unmodified cytochrome b_5 and cytochrome c is essentially the same in either complex. In contrast, the electrostatic interaction energies of DME-cytochrome b_5 with cytochrome c in either complex are isoenergetic at low pH (6.75) and diverge at higher pH values in favor of the off-edge geometry (Figure 6A). On the basis of electrostatic stability alone, the calculations do not predict a dominant protein–protein interaction but rather a mixture of complexes whose relative populations shift with pH. The $pK_{1/2}$ values that were calculated for the titrating residues of cytochrome b_5 and DME-cytochrome b_5 are reported for both complex geometries in Table I. The $pK_{1/2}$ value for His-26 is sensitive to heme propionate esterification and the association geometry with cytochrome c. Reducing the negative potential at His-26 by propionate esterification or docking with the positively charged cytochrome c is expected to decrease the $pK_{1/2}$ value. However, when the cytochrome c is located such that the protein–protein interface is in close proximity to His-26, the predicted $pK_{1/2}$ value increased to 7.6. The interaction of His-26 with several nearby anionic

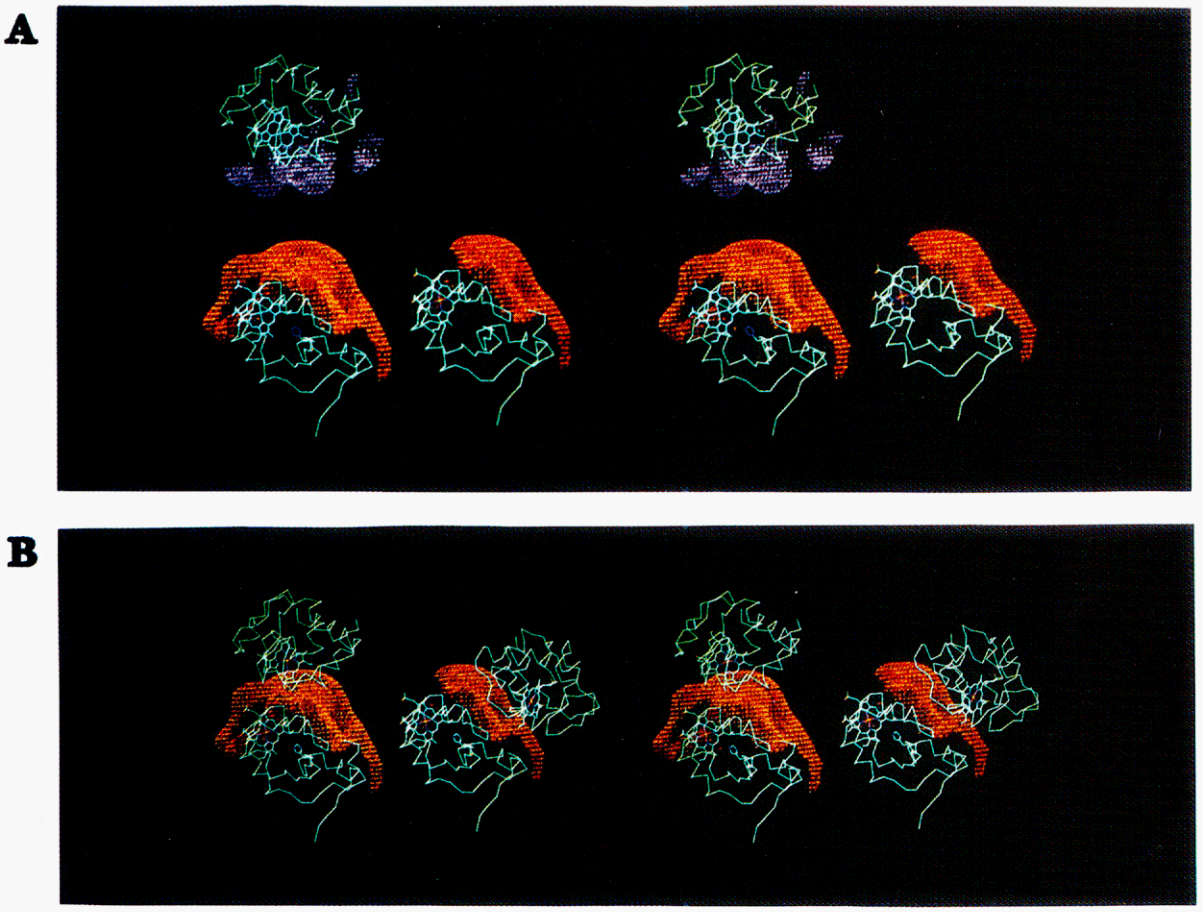

FIGURE 5: (A) Stereo diagram of positive electrostatic potential surfaces (4 kT) calculated for cytochrome *c* (upper right) and negative potential surfaces for trypsin-solubilized native cytochrome b_5 (right) and DME-cytochrome b_5 (left) at pH 7.6, I = 4 mM, 25 °C. The side chain of His-26 is included. (B) Stereo diagram of the electrostatic potentials (−4 kT) for native and DME-cytochrome b_5 with the cytochrome *c* α-carbon backbone, indicating the electrostatically preferred complex geometry under the same solution conditions as assumed in (A).

residues at the protein interface is enhanced by a reduction in their solvent accessibility.

Discussion

The experimental approach employed in this work is similar to that used in a large number of studies involving specifically modified derivatives of cytochrome *c* to assess the role of individual amino acid residues in interaction of cytochrome *c* with other redox-active proteins [e.g., Osheroff et al. (1980a,b) and Smith et al. (1977, 1980)]. In these previous studies, however, protein–protein interactions are examined by determining the effect of specific chemical modifications on steady-state kinetic results rather than by direct determination of stability of complex formation. In addition, these previous studies generally involved incorporation of fairly substantial derivatizing groups into the protein, e.g., trinitrophenyl, monocarboxydinitrophenyl, trifluoroacetyl, and trifluoromethylphenylcarbamoyl groups. Our approach, therefore, differs in that we have attempted to study protein–protein binding independent of electron transfer and we have employed a relatively minor chemical modification. We note, nonetheless, that the resulting propionate methyl ester is not isosteric with the native structure.

We have shown that both native and heme-substituted cytochrome b_5 form a 1:1 complex with cytochrome *c*. Their interactions with cytochrome *c* show similar dependencies on ionic strength (Figure 4). The results shown in Figure 3 demonstrate that esterification of the heme propionates does not diminish the maximum observed stability of complex formation between the cytochromes. Esterification of the heme propionates does, however, shift the pH optimum for complex formation to higher pH and gives a slightly more stable final complex with cytochrome *c*. This finding is contrary to the expectation that loss of one of the intermolecular salt links would decrease the stability of the cytochrome b_5–cytochrome *c* complex. Our model building and experimental data, when taken together, are consistent with an electrostatically driven association of cytochrome *c* and cytochrome b_5 (i.e., a 1:1 complex between cytochrome *c* and both native and esterified cytochrome b_5 that is stabilized by long- and short-range electrostatic forces arising from the unique surface-charge distribution of each protein and the formation of intermolecular linkages); however, the geometric details of the complex are predicted to depend on solution pH and ionic strength.

Figure 5 shows the calculated electrostatic potential surfaces for native cytochrome b_5 and DME-cytochrome b_5. Both molecules possess negatively charged electrostatic potential surfaces. Neutralization of the two negatively charged propionates decreases the extent of the electrostatic potential surface for cytochrome b_5 and shifts its center away from the exposed heme edge. Computer graphic modeling of the interaction between cytochrome b_5 and cytochrome *c* indicates that a number of protein–protein complexes that maintain the overlap of oppositely charged electrostatic potential surfaces are possible.

The observed pH dependencies of the protein–protein association constants are bell-shaped and display pH optima between 7.5 and 8.5. The increase in association constant as the pH is raised can be understood as a shift in complex populations as His-26 of cytochrome b_5 is deprotonated. For

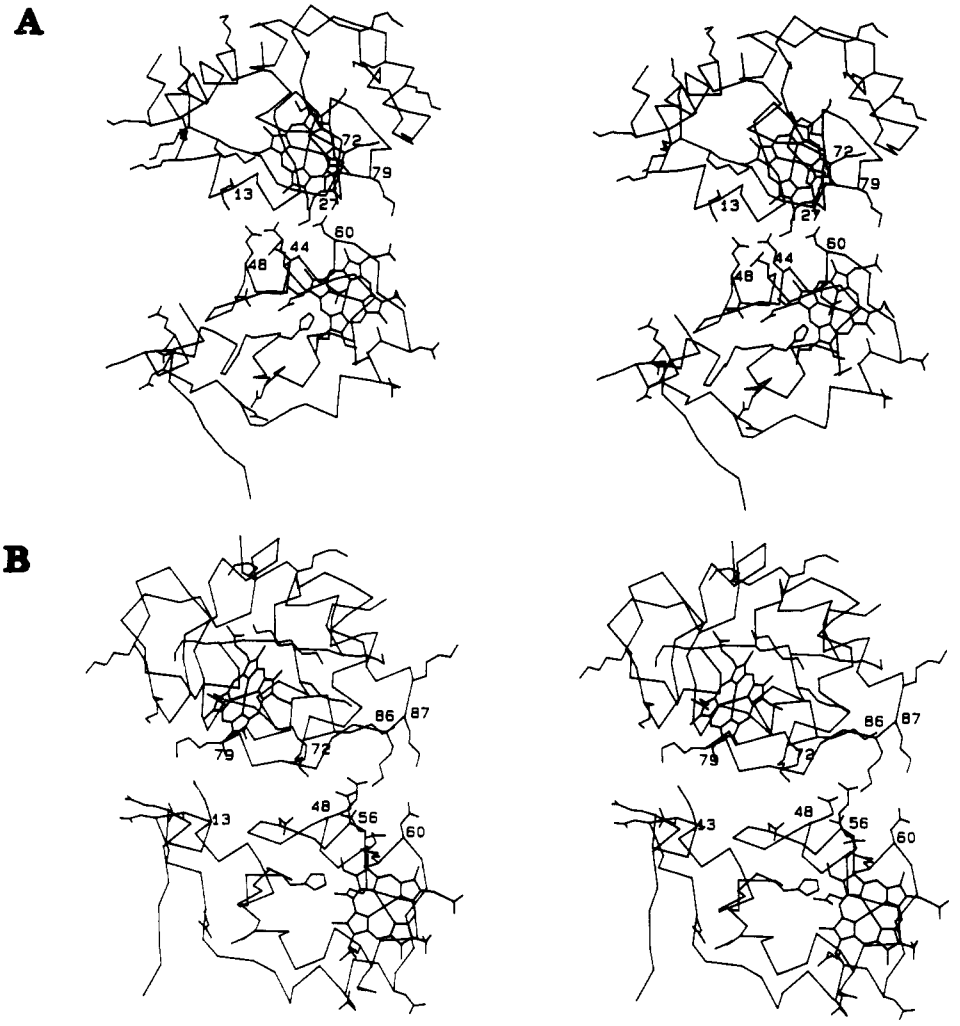

FIGURE 6: (A) Stereoscopic view of a molecular complex modeled to maximize overlap between oppositely charged electrostatic potential surfaces of cytochrome *c* and DME-cytochrome b_5. Lysyl residues 72, 79, 86, and 87 are respectively salt-linked to residues Glu-48, Glu-13, Glu-56, and Asp-60 of cytochrome b_5. (B) Stereoscopic view of the electron-transfer complex between cytochrome b_5 and cytochrome *c* proposed by Salemme (1976). Intermolecular salt linkages are formed between lysyl residues 13, 27, 72, and 79 of cytochrome *c* and Glu-48, Glu-44, Asp-60, and a heme propionate of cytochrome b_5, respectively. The α-carbon backbone and all atoms of the heme prosthetic groups are shown for both cytochromes in each model. In addition, all pertinent lysyl side chains on cytochrome *c* (upper molecule) and all relevant aspartyl and glutamyl side chains on cytochrome b_5 (lower molecule) are shown. The side chain of His-26 on cytochrome b_5 is also included. Residue numbering for cytochrome b_5 is that of Mathews et al. (1972). Intermolecular salt-link distances are 2.9–3.1 Å in each case.

the interaction between DME-cytochrome b_5 and cytochrome *c*, the deprotonation of His-26 makes the off-edge complex the electrostatically preferred complex. For the interaction between unmodified cytochrome b_5 and cytochrome *c*, the heme edge complex is favored at low pH and the deprotonation of His-26 leads to the two binding geometries being isoenergetic. As the $pK_{1/2}$ value for His-26 in the off-edge geometry with cytochrome *c* is predicted to be 7.3 and 7.6 for unmodified cytochrome b_5 and DME-cytochrome b_5 respectively, the interaction between either form of cytochrome b_5 and cytochrome *c* is expected to exhibit a similar dependence on pH with a midpoint at lower apparent p*K* for the unmodified cytochrome b_5–cytochrome *c* interaction. The calculations suggest two possibilities for the decrease in K_a as the pH is raised further. The deprotonation of the amino terminus of cytochrome b_5 can lead to another shift in the mixture of geometries favored for the association of cytochrome *c*, and/or the increasing net charge on cytochrome b_5 at higher pH leads to destabilization of the isolated protein and may interfere with the entropy of docking.

The computer modeling results for cytochrome b_5 and cytochrome *c* imply that the interaction geometry between proteins whose association is electrostatically driven can depend significantly on solvent conditions such as pH and ionic strength. A variety of complexes may exist transiently in solution, of which a small number may represent productive precursor complexes for electron transfer. In other words, the static models that have been developed to represent electron-transfer complexes of heme proteins are best regarded as apparent minima in the free energy surface for complex formation that probably possesses several nearly isoenergetic minima. The rate and mechanism of interconversion between possible complexes are not easily examined. If a protein pair must separate by a few angstroms to migrate across each others surface, the electrostatic energy barrier is likely to be several kilocalories per mole. However, if the proteins can walk across each others surface, making and breaking ion pairs (see Figure 6), then the electrostatic barrier is 1 kcal/mol or less. It is possible, nevertheless, that steric constraints may offset the energetic advantage of the latter mechanism.

The most obvious question regarding the two complexes proposed here concerns the difference in rate of intramolecular electron transfer that each should exhibit. On the basis of current theories (Scott et al., 1985), electron transfer is expected to be significantly slower within the off-edge complex owing to the increase in heme iron to heme iron distance and

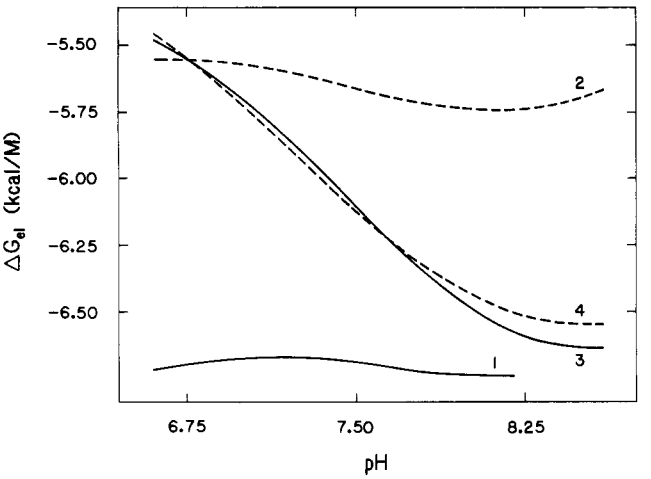

FIGURE 7: Calculated energy of complex formation for native proteins in the orientation proposed by Salemme (curve 1) and in the alternative orientation (curve 3) and for the DME-cytochrome b_5–cytochrome c complex in orientation proposed by Salemme (curve 2) and in the alternative orientation (curve 4) (I = 4 mM, 25 °C).

the non-coplanar orientation of the heme prosthetic groups in this docking geometry.

Registry No. Cytochrome c, 9007-43-6; cytochrome b_5, 9035-39-6; heme, 14875-96-8.

REFERENCES

Bernstein, F. C., Koetzle, T. F., Williams, G. J. B., Meyer, E. F., Jr., Brice, M. D., Rodgers, J. R., Kennard, O., Schimanouchi, T., & Tasume, M. (1977) *J. Mol. Biol. 112*, 535.

Dayhoff, M. O. (1972) *Atlas of Protein Sequence and Structure*, Vol. 5, p D-7, National Biomedical Research Foundation, Washington, DC.

Eley, C. G. S., & Moore, G. R. (1983) *Biochem. J. 215*, 11.

Mathews, F. S., Levine, M., & Argos, P. (1972) *J. Mol. Biol. 64*, 449.

Mathews, F. S., Czerwinski, E. W., & Argos, P. (1979) in *The Porphyrins* (Dolphin, D., Ed.) Vol. 7, p 107, Academic Press, New York.

Matthew, J. B. (1985) *Annu. Rev. Biophys. Biophys. Chem. 14*, 387.

Matthew, J. B., & Richards, F. M. (1982) *Biochemistry 21*, 4989.

Matthew, J. B., Friend, S. H., Botelho, L. H., Lehman, L. D., Hanania, G. I. H., & Gurd, F. R. N. (1978) *Biochem. Biophys. Res. Commun. 81*, 416.

Matthew, J. B., Weber, P. C., Salemme, F. R., & Richards, F. M. (1983) *Nature (London) 301*, 169.

Mauk, M. R., Reid, L. S., & Mauk, A. G. (1982) *Biochemistry 21*, 1843.

Mauk, A. G., Mauk, M. R., Weber, P. C., & Matthew, J. B. (1985) *Fed. Proc., Fed. Am. Soc. Exp. Biol. 44*, 1780.

McLendon, G. L., Winkler, J. R., Nocera, D. G., Mauk, M. R., Mauk, A. G., & Gray, H. B. (1985) *J. Am. Chem. Soc. 107*, 739.

Ng, S., Smith, M. B., Smith, H. T., & Millett, F. (1977) *Biochemistry 16*, 4975.

Osheroff, N., Brautigan, D. L., & Margoliash, E. (1980a) *J. Biol. Chem. 255*, 8245.

Osheroff, N., Brautigan, D. L., & Margoliash, E. (1980b) *Proc. Natl. Acad. Sci. U.S.A. 77*, 4439.

Reid, L. S., & Mauk, A. G. (1982) *J. Am. Chem. Soc. 104*, 841.

Reid, L. S., Mauk, M. R., & Mauk, A. G. (1984) *J. Am. Chem. Soc. 106*, 2182.

Salemme, F. R. (1976) *J. Mol. Biol. 102*, 563.

Salemme, F. R. (1977) *Annu. Rev. Biochem. 46*, 299.

Scott, R. A., Mauk, A. G., & Gray, H. B. (1985) *J. Chem. Educ. 62*, 932.

Smith, H. T., Staudenmayer, N., & Millett, F. (1977) *Biochemistry 16*, 4971.

Smith, M. B., Stonehuerner, J., Ahmed, A. J., Staudenmayer, N., & Millett, F. (1980) *Biochim. Biophys. Acta 592*, 303.

Stonehuerner, J., Williams, J. B., & Millet, F. (1979) *Biochemistry 18*, 5422.

Strittmatter, P., & Ozols, J. (1966) *J. Biol. Chem. 241*, 4787.

Swanson, R., Trus, B. L., Mandel, N., Mandel, G., Kallai, O., & Dickerson, R. E. (1977) *J. Biol. Chem. 252*, 759.

Takano, T., & Dickerson, R. E. (1981a) *J. Mol. Biol. 153*, 79.

Takano, T., & Dickerson, R. E. (1981b) *J. Mol. Biol. 153*, 95.

Weber, P. C., & Tollin, G. (1985) *J. Biol. Chem. 260*, 5568.

Wherland, S., & Gray, H. B. (1976) *Proc. Natl. Acad. Sci. U.S.A. 73*, 2950.